UNCERTAINTY QUANTIFICATION IN HIERARCHICAL VEHICULAR FLOW MODELS

Michael Herty and Elisa Iacomini*

RWTH Aachen University
Institut für Geometrie und Praktische Mathematik
Templergraben 55, 52062 Aachen, Germany

(Communicated by Shi Jin)

Abstract. We consider kinetic vehicular traffic flow models of BGK type [24]. Considering different spatial and temporal scales, those models allow to derive a hierarchy of traffic models including a hydrodynamic description. In this paper, the kinetic BGK–model is extended by introducing a parametric stochastic variable to describe possible uncertainty in traffic. The interplay of uncertainty with the given model hierarchy is studied in detail. Theoretical results on consistent formulations of the stochastic differential equations on the hydrodynamic level are given. The effect of the possibly negative diffusion in the stochastic hydrodynamic model is studied and numerical simulations of uncertain traffic situations are presented.

1. **Introduction.** The mathematical description of vehicular traffic flow is possible at different spatial and temporal scales ranging from models for individual cars [17] up to a description of aggregated quantities like the traffic density [3, 11, 16, 33]. Recent works present models on those scales as well as methods to traverse the existing hierarchy, see e.g. [1, 4, 12, 15, 23, 25] and references therein. We are particularly interested in two scales, the hydrodynamic or fluid–like models for aggregated quantities and a statistical description of traffic as e.g. proposed in [6, 22, 28, 29]. Our contribution is mainly based on the recently introduced hierarchy [24] where in particular a class of BGK (Bhatnagar, Gross and Krook [5]) models have been considered. The fluid–like models considered are second-order Aw-Rascle-Zhang type models [1, 49]. The hierarchy presented in [24] has been deterministic assuming that all model parameters and initial data are known exactly. However, often there is need to take uncertainties into account, e.g. due to noisy measurements and due to variations in the behavior of vehicular traffic leading to uncertainties. Then, it is necessary to extend the concepts to the stochastic case to consider probability laws or statistical moments. The treatment of stochastic models can be either non–intrusive, e.g., based on sampling (Monte–Carlo) [32, 41, 42] or based on collocation [2], or intrusive [31, 46]. In the later approach, stochastic input is represented by a series of orthogonal functions, known as generalized polynomial chaos (gPC) expansions [7, 45, 47], substituted in the governing equations and then

*Corresponding author: Elisa Iacomini.

projected using a Galerkin projection. We follow this intrusive approach in order to investigate how uncertainty propagates between the kinetic and the fluid flow hierarchy of description. The possible links are depicted in Figure 1. Recently, results using the intrusive approach for kinetic equations have been presented and we refer to [8, 9, 26, 27, 40, 48, 50] for corresponding results. For hyperbolic models on the fluid type description there have also been recent results [10, 14, 18, 20, 21, 35, 37, 30] – mostly centered at the question of hyperbolicity of the underlying gPC expanded system of partial differential equations. For the presented investigation we in particular refer to [19] where a gPC expansion for the Aw-Rascle-Zhang has been established. Therein, it has been shown that for a particular choice of orthogonal functions, the resulting expanded system is hyperbolic, see [19, Theorem 2.2]. In this paper we will investigate the link between stochastic BGK and stochastic second order traffic flow models. In [24] the diffusivity coefficient has been used to classify possible unstable traffic regimes. We will show that the discussion translates to the stochastic case and allows to characterize possible traffic zones of high risk. Here, we also investigate the dynamic case compared with the previous publication. Our presentation follows the diagram shown in Figure 1, in particular, the indicated blue connections.

The propagation of uncertainty through hierarchies has also been explored e.g. in the case of the Vlasov-Poisson-Fokker-Planck system [27]. Contrary to the approach here, however, the resulting diffusive system has been shown to be well–posed without further assumptions. Due to the nonlinear hyperbolic structure the presented results therein do not extend directly to the present case. Moreover, uncertainty across different scales of observation is investigated in [44], where a different equilibrium density has been derived. Also, in [43] the propagation of uncertainty is discussed but the origin and treatment of uncertainty is very different to the presented work.
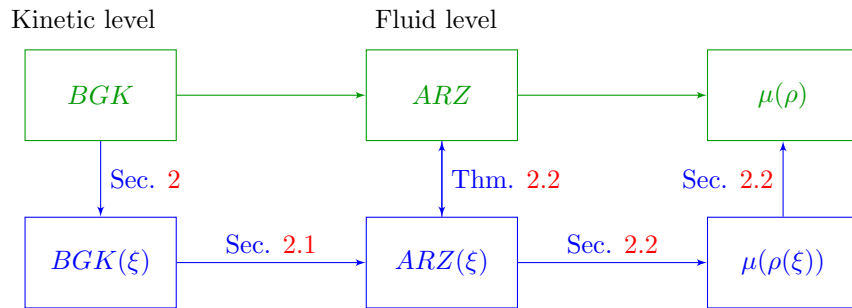

FIGURE 1. Outline of the model hierarchy. The left two columns indicate the kinetic and fluid description of traffic flow as presented in [24]. The third column refers to the diffusion coefficient $\mu(\rho)$ to classify traffic instabilities. The green hierarchy is deterministic while the blue includes a parametric uncertainty ξ. The indicated links are established in this paper.

2. **Hierarchical stochastic traffic flow models.** A kinetic traffic flow model reads

$$\partial_t f(t,x,v) + v\partial_x f(t,x,v) = \frac{1}{\varepsilon}Q[f,f](t,x,v), \qquad (1)$$

where $f(t, x, v) : \mathbb{R}^+ \times \mathbb{R} \times [0, V_M] \to \mathbb{R}^+$ is the mass distribution function of traffic. The operator Q encodes the detailed car–to–car interactions and it will be modeled in the following as a linear operator of BGK type. The quantity ε is positive, and yields a relaxation rate weighting the relative strength between the convective term and source term. The spatial variable is denoted by $x \in \mathbb{R}$ and the velocity v is assumed to be bounded by zero and a maximum speed V_M. Finally, $t \geq 0$ is the time and we assume w.l.o.g. that the initial datum $f_0(x, v)$ is such that the density ρ_0 is bounded by one, i.e.,

$$\int_0^{V_M} f_0(x, v)dv =: \rho_0(x) \leq 1 \; \forall x \in \mathbb{R}. \tag{2}$$

BGK type collision operators prescribe a relaxation to equilibrium at rate ε. In the space homogeneous case, the equilibrium is characterize by a function $M_f(v; \rho)$ called Maxwellian possibly depending on $\rho = \rho_0$. The Maxwellian defines the mean speed of vehicles at equilibrium through the relation

$$U(\rho) = \frac{1}{\rho} \int_0^{V_M} v M_f(v; \rho)dv. \tag{3}$$

The precise modeling of Q as well as the existence of suitable Maxwellians has been discussed intensively in the literature and we refer e.g. to [24, 38]. Integrating equation (1) in velocity space, and provided that $\int_0^{V_M} Q[f, f]dv = 0$, and one obtains the evolution equation for the density $\rho(t, x) = \int_0^{V_M} f(t, v, x)dv$ as

$$\partial_t \rho(t, x) + \partial_x \left(\int_0^{V_M} v f(t, x, v)dv \right) = 0. \tag{4}$$

If the system approaches equilibrium, $f \to M_f$, then

$$\partial_t \rho(t, x) + \partial_x \left(\rho(t, x) U(\rho(t, x)) \right) = 0. \tag{5}$$

The previous equation and the initial data $\rho(0, x) = \rho_0(x)$ provides a level of description on an aggregated, fluid–like level. If, however, the system is not at equilibrium, the equation (4) is still coupled to the kinetic equation (1). In the case $\varepsilon \to 0$, the interactions of cars are so frequent to instantaneously relax f to the local equilibrium distribution M_f. Instead, we expect that if $\varepsilon > 0$ is small but positive, we are in a regime where the kinetic equation is given by an extended continuum hydrodynamic system of equations as for example the Aw-Rascle and Zhang model [1, 49]. Studying stability properties of traffic patterns in terms of an asymptotic analysis in terms of the parameter ε has been conducted e.g. [24, 39] using a Chapman-Enskog expansion. The Aw–Rascle–Zhang equations are a system of hyperbolic equations for traffic density ρ and (average) velocity $v = v(t, x) = \frac{q(t,x)}{\rho(t,x)}$ for $\rho > 0$. Here, $q(t, x)$ is the flux. Moreover in the Aw–Rascle–Zhang model, the function $h(\rho) : \mathbb{R}^+ \to \mathbb{R}^+$ is introduced and is an increasing, differentiable function of the density called hesitation or pressure function [16].
For some given equilibrium velocity $V^{eq} : \mathbb{R}^+ \to \mathbb{R}^+$ decreasing in its argument, the equations read for $\rho = \rho(t, x)$ and $q = q(t, x)$ with $x \in \mathbb{R}, t \in \mathbb{R}^+$:

$$\partial_t \rho + \partial_x (q - \rho h(\rho)) = 0, \tag{6}$$

$$\partial_t q + \partial_x \left(\frac{q^2}{\rho} - q h(\rho) \right) = \frac{1}{\epsilon} \left(\rho V_{eq}(\rho) + \rho h(\rho) - q \right). \tag{7}$$

In the limit $\epsilon \to 0$ we formally obtain a (first–order) consistent approximation of solutions to (6) to (4) by defining for $\rho \geq 0$

$$V^{eq}(\rho) = U(\rho). \tag{8}$$

In the following we are interested in the link between (6) and (1), resp. (11) in the *stochastic case*. A key observation in the deterministic analysis [24] has been the link between a discretization of the kinetic equation (1) using a finite number of particles and the Aw–Rascle–Zhang traffic flow model. This connection has been established using the variable $w \in W = [w_{\min}, \infty)$

$$w = v + h(\rho). \tag{9}$$

Here, $w_{\min} = h(0)$. For $h(\rho)$, we assume that for $\gamma \in \{1, 2\}$

$$h(\rho) = \rho^\gamma. \tag{10}$$

The quantity of w can be understood as a driver's preference that is Lagrangian quantity [1, Section 4]. Based on a particle description the link between the kinetic equation for $g : \mathbb{R}^+ \times \mathbb{R} \times W \to \mathbb{R}^+$ is

$$\partial_t g(t, x, w) + \partial_x \Big[(w - h(\rho(t, x)))g(t, x, w)\Big] = \frac{1}{\varepsilon}\Big(M_g(w; \rho(t, x)) - g(t, x, w)\Big), \tag{11}$$

and the Aw–Rascle–Zhang equations (6) for the density ρ and flux q

$$\rho(t, x) = \int_W g(t, x, w)dw, \qquad q(t, x) = \int_W w\, g(t, x, w)dw \tag{12}$$

have been established using asymptotic analysis in ε. The Maxwellian M_g can be related to M_f, which is assumed to fulfill for any $\rho \in \mathbb{R}$

$$\int_W M_g(w; \rho)\, dw = \rho, \tag{M1}$$

$$\int_W w\, M_g(w; \rho)\, dw = \rho V_{eq}(\rho) + \rho h(\rho). \tag{M2}$$

The function $V_{eq} : \mathbb{R} \to \mathbb{R}_0^+$ is the previously introduced equilibrium velocity. As discussed we are interested in the description of vehicular traffic on the kinetic (11) and fluid–dynamic (6) level in the presence of parametric uncertainty ξ. This uncertainty may have many origins but for now we simply assume that it can be described by a (possibly multi-dimensional) random variable ω. Let the random variable ω be defined on the probability space $(\Omega_\omega, \mathcal{F}(\Omega), \mathbb{P})$. Further, we denote by $\xi = \xi(\omega) : \Omega_\omega \to \Omega \subset \mathbb{R}^d$ a (possibly d-dimensional) real-valued random variable. Assume further that ξ is absolutely continuous with respect to the Lebesgue measure on $\mathbb{R}^d$ and denote by $p_\Xi(\xi) : \Omega \to \mathbb{R}_+$ the probability density function of ξ. For simplicity we assume that the uncertainty enters only in the initial data $g_0(x, w, \omega)$ that is now random field defined on $\mathbb{R} \times W \times \Omega_\omega$ that is denoted by $g_0(x, w, \xi) = g_0(x, w, \xi(\omega)) : \mathbb{R} \times W \times \Omega \to \mathbb{R}$. Further, we assume that $g_0(x, w, \cdot) \in L^2(\mathbb{R}^d, p_\Xi)$ a.e. in (x, w). Then, we are interested in the evolution of the random field $g(t, x, w, \xi) : \mathbb{R}^+ \times \mathbb{R} \times W \times \Omega$ governed by a BGK–kinetic equation (11) with uncertain initial data g_0. For the following derivations it is sufficient to assume that first and second moment g w.r.t. to ω exist as well as up to second moment in ξ. Further, the derivation is based on the assumption that the random field g fulfills (13) pointwise a.e. in (t, x, w) as well as p_Ξ a.s. in ξ :

$$\partial_t g(t,x,w,\xi) + \partial_x\Big[(w - h(\rho(t,x,\xi)))g(t,x,w,\xi)\Big] = \frac{1}{\varepsilon}\Big(M_g(w;\rho(t,x,\xi)) - g(t,x,w,\xi)\Big),$$
$$\tag{13}$$

$$g(0,x,w,\xi) = g_0(x,w,\xi),$$
$$\tag{14}$$

$$\rho(t,x,\xi) = \int_W g(t,x,w,\xi)dw.$$
$$\tag{15}$$

Next, we turn to the description of the intrusive approach in order to establish the hierarchy indicated in Figure 1. A random field $g(t,x,w,\cdot) \in L^2(\Omega, p_\Xi)$ can be expressed by a spectral expansion [7]

$$g(t,x,w,\xi) = \sum_{k=0}^{\infty} \tilde{g}_i(t,x,w)\phi_i(\xi),$$
$$\tag{16}$$

where $\phi_i \in L^2(\Omega, p_\Xi)$ are basis functions, typically chosen orthonormal with respect to the weighted scalar product, and $\{\tilde{g}_i(t,x,w)\}_{i=0}^{\infty}$ is a set of coefficients:

$$\tilde{g}_i(t,x,w) = \int_\Omega g(t,x,w,\xi)\phi_i(\xi)p_\Xi(\xi)d\xi.$$
$$\tag{17}$$

The previous expansion is truncated at K to obtain an approximation with $K+1$ moments. The projection of $g(t,x,w,\cdot)$ to the span of the $K+1$ base functions is denoted by

$$G_K(g(t,x,w,\cdot))(\xi) := \sum_{i=0}^{K} \tilde{g}_i(t,x,w)\phi_i(\xi) \quad a.e.\ \xi \in \Omega.$$
$$\tag{18}$$

The expansion (16) is called generalized polynomial chaos expansion (gPC). In particular, for kinetic equations, also more involved than the given BGK equation, this has been explored recently in a series of papers, see e.g. [8, 9, 26, 27, 40, 48, 50]. Therein, also conditions on $\{g_{0,i}\}_{i=0}^{\infty}$ have been developed to allow for existence of a (weak) stochastic solution g.

Next, we establish the connection between the random BGK model (11) and the stochastic Aw–Rascle–Zhang system. Assume g is a pointwise a.e. and integrable solution to the system (13). Then, the density ρ and the flux q allow for gPC expansion for all $i \in \mathbb{N}$:

$$\rho(t,x,\xi) = \int_W g(t,x,w,\xi)dw = \sum_{i=0}^{\infty} \tilde{\rho}_i\phi_i(\xi),\ \tilde{\rho}_i = \tilde{\rho}_i(t,x) = \int_W \tilde{g}_i(t,x,w)dw,$$
$$\tag{19}$$

$$q(t,x,\xi) = \int_W wg(t,x,w,\xi)dw = \sum_{i=0}^{\infty} \tilde{q}_i\phi_i(\xi),\ \tilde{q}_i = \tilde{q}_i(t,x) = \int_W w\tilde{g}_i(t,x,w)dw.$$
$$\tag{20}$$

As in [20, 35, 36] we introduce the Galerkin production for any finite $K > 0$ and any $u, z \in L^2(\Omega, p_\Xi)$, $\tilde{u} = (\tilde{u}_i)_{i=0}^{K}$, $\tilde{z} := (\tilde{z}_i)_{i=0}^{K}$ and for all $i, j, \ell = 0, \ldots, K$:

$$\mathcal{G}_K[u,z](t,x;\xi) := \sum_{k=0}^{K} (\tilde{u} * \tilde{z})_k(t,x)\phi_k(\xi),$$

$$(\tilde{u} * \tilde{z})_k(t,x) := \sum_{i,j=0}^{K} \tilde{u}_i(t,x)\tilde{z}_j(t,x)\mathcal{M}_\ell,$$

$$(\mathcal{M}_\ell)_{i,j} := \int_\Omega \phi_i(\xi)\phi_j(\xi)\phi_\ell(\xi)p_\Xi(\xi)d\xi.$$

Note that $\mathcal{M}_\ell$ is a symmetric matrix of dimension $(K+1) \times (K+1)$ for any fixed $\ell \in \{0,\dots,K\}$. The Galerkin product $\mathcal{G}_K$ is not the only possible projection of the product of random variables u, z on the subspace $span\{ \phi_0, \dots, \phi_K\}$. However, this choice (and additional assumptions on the base functions) have shown to be sufficient to guarantee hyperbolicity of the $p-$system [20] as well as the Aw–Rascle–Zhang system [19]. Furthermore, we have $\tilde{u} * \tilde{z} = \mathcal{P}(\tilde{u})\tilde{z}$ for $\mathcal{P} \in \mathbb{R}^{K+1 \times K+1}$ and $\tilde{u} \in \mathbb{R}^{K+1}$ defined by

$$\mathcal{P}(\tilde{u}) := \sum_{\ell=0}^{K} \tilde{u}_\ell \mathcal{M}_\ell. \tag{21}$$

The Galerkin product is symmetric, but not associative [13, 34, 41]. Finally, we assume that the chosen functions $\{\phi_i\}_i$ fulfill the following properties [18, A1-A3]

(A1) The matrices $\mathcal{M}_\ell$ and $\mathcal{M}_k$ commute for all $\ell, k = 0, \dots, K$.
(A2) The matrices $\mathcal{P}(\hat{u})$ and $\mathcal{P}(\tilde{z})$ commute for all $\tilde{u}, \tilde{z} \in \mathbb{R}^{K+1}$.
(A3) There is an eigenvalue decomposition $\mathcal{P}(\tilde{u}) = V\mathcal{D}(\tilde{u})V^T$ with constant eigenvectors V.

It has been shown that for example the one–dimensional Wiener–Haar basis and piecewise linear multiwavelets fulfill the previous assumptions, but, Legendre and Hermite polynomials do *not* fulfill those requirements.

Similar to [26, 40] and for any fixed K we derive a system of equations for the evolution of $\tilde{g}_i(t,x,w) : \mathbb{R}^+ \times \mathbb{R} \times W \to \mathbb{R}$ for $i = 0, \dots, K$ by projection the operators of equation (13) to the space $span\{\phi_i : i = 0, \dots, K\}$. We further assume that the set of base functions is orthonormal and fulfills the assumptions (A1)–(A3).

$$\partial_t \, \tilde{g}_i(t,x,w) + \partial_x \left(\left(wId - \mathcal{P}\left(h(\tilde{\rho}(t,x))\right)\right)\tilde{g}(t,x,w) \right)_i = \frac{1}{\varepsilon}\left(\widetilde{M}_i\left(w; \tilde{\rho}(t,x)\right) - \tilde{g}_i(t,x,w) \right), \tag{22}$$

$$\tilde{g}_i(0,x,w) = \int_\Omega g_0(t,x,w,\xi)\phi_i(\xi)p_\Xi(\xi)d\xi \tag{23}$$

In the derivation of the previous system (22) we have used the following results: Under assumptions (A1)-(A3) h, as given by equation (10), fulfills [19]:

$$\sum_{j=0}^{K} \int_\Omega h\left(\sum_{\ell=0}^{K} \tilde{\rho}_\ell \phi_\ell(\xi) \right) \tilde{g}_j \phi_j(\xi)\phi_i(\xi)p_\Xi(\xi)d\xi = \left(\mathcal{P}(h(\tilde{\rho}))\tilde{g}\right)_i, \ \forall i = 0, \dots, K. \tag{24}$$

Further, we define for $i = 0, \dots, K$

$$\widetilde{M}_i\left(w; \tilde{\rho}(t,x)\right) := \int_\Omega M_g\Big(w; \sum_{\ell=0}^K \tilde{\rho}_\ell(t,x)\phi_\ell(\xi)\Big)\phi_i(\xi)p_\Xi dw d\xi, \tag{25}$$

$$\widehat{M}_g(w, \tilde{\rho}(t,x), \xi) := M_g\left(w; \sum_{i=0}^K \tilde{\rho}_i(t,x)\phi_i(\xi)\right). \tag{26}$$

2.1. **Derivation of stochastic Aw–Rascle–Zhang model.** In [24] a connection between two levels of description, i.e., (11) and (6) has been established under the assumption that the Maxwellian fulfills (M1) and (M2). The next lemma shows that those assumptions extend directly to the stochastic case.

Lemma 2.1. *Let $K > 0$. Consider a base functions ϕ_i and $i = 0,\dots,K$ fulfilling (A1)–(A3). Furthermore, assume that the functions M_g, V^{eq} fulfill the assumptions (M1)-(M2). Let g be expanded in a gPC series with $K+1$ modes as given by equation (16). Then, $\widetilde{M}_g$ defined by (26) fulfill for any $i = 0,\dots,K$, $t \geq 0$, and $x \in \mathbb{R}$:*

$$\int_W \widetilde{M}_i\left(w; \tilde{\rho}(t,x)\right) \, dw = \tilde{\rho}_i(t,x), \tag{UM1}$$

$$\int_W w \, \widetilde{M}_i\left(w; \tilde{\rho}(t,x)\right) dw = \Big(\mathcal{P}(V_{eq}(\tilde{\rho}(t,x)))\tilde{\rho}(t,x) + \mathcal{P}(h(\tilde{\rho}(t,x)))\tilde{\rho}(t,x)\Big)_i. \tag{UM2}$$

Proof. Due to (M1)-(M2) and (19) we obtain for a.e. $(t,x,\xi) \in \mathbb{R}^+ \times \mathbb{R} \times \Omega$.

$$\int_W M_g(w; \rho(t,x,\xi)) \, dw = \rho(t,x,\xi), \tag{27}$$

$$\int_W w \, M_g(w; \rho(t,x,\xi)) \, dw = \rho(t,x,\xi)V_{eq}(\rho(t,x,\xi)) + \rho(t,x,\xi)h(\rho(t,x,\xi)). \tag{28}$$

Integration with respect to dw yields

$$\int_W \widetilde{M}_i(w, \tilde{\rho}(t,x)) \, dw = \int_\Omega \int_W M_g\Big(w; \sum_{j=0}^K \tilde{\rho}_j(t,x)\phi_j(\xi)\Big)\phi_i(\xi)dw p_\Xi(\xi)d\xi =$$

$$\int_\Omega \sum_{j=0}^K \tilde{\rho}_j(t,x)\phi_j(\xi)\phi_i(\xi)p_\Xi(\xi)d\xi = \tilde{\rho}_i(t,x).$$

The similar computation yielding (UM2) is omitted. □

In the following result we derive a gPC formulation of the fluid model obtained by the stochastic BGK model (13). Further, we compare this model with the stochastic Aw–Rascle–Zhang model derived in [19]. The theorem shows that under assumption (29) the derived gPC model is equivalent to the stochastic model of [19]. Therein, it has also been shown that the partial differential equation is hyperbolic.

Theorem 2.2. *Let $K > 0, \epsilon > 0$. Assume the base functions $\{\phi_0, \dots, \phi_K\}$ fulfill (A1)–(A3) and assume that the functions M_g, V^{eq} fulfill the assumptions (M1)-(M2) and let $h(\cdot)$ fulfill (10). Let $\tilde{g}_i$ be a strong solution to (22) and (25) for $i = 0,\dots,K$. Further, assume that for $i = 0,\dots,K$ and $(t,x) \in \mathbb{R}^+ \times \mathbb{R}$*

$$\int_W w^2 \, \tilde{g}_i(t,x,w)dw = (\mathcal{P}(\tilde{q}(t,x))\mathcal{P}^{-1}(\tilde{\rho}(t,x))\tilde{q}(t,x))_i, \qquad (29)$$

where $(\tilde{\rho}, \tilde{q})_i$ are the first and second moment of $\tilde{g}_i$ as in (19)–(20) and $\mathcal{P}$ is defined by (21).

Then, the functions $(\tilde{\rho}, \tilde{q})$ formally fulfill pointwise in $(t,x) \in \mathbb{R}^+ \times \mathbb{R}$ and for all $i = 0, \ldots, K$ the second–order traffic flow model

$$\partial_t \tilde{\rho}_i(t,x) + \partial_x \left[\tilde{q}_i(t,x) - (\mathcal{P}(\tilde{\rho}(t,x))\tilde{\rho}(t,x))_i \right] = 0 \qquad (30a)$$

$$\partial_t \tilde{q}_i(t,x) + \partial_x \left[(\mathcal{P}(\tilde{q}(t,x))\mathcal{P}^{-1}(\tilde{\rho}(t,x))\tilde{q}(t,x))_i - (\mathcal{P}(\tilde{\rho}(t,x))\tilde{q}(t,x))_i \right] = \qquad (30b)$$

$$\frac{1}{\epsilon}\left(\left(\mathcal{P}(V_{eq}(\tilde{\rho}(t,x)))\tilde{\rho}(t,x) + \mathcal{P}(h(\tilde{\rho}(t,x)))\tilde{\rho}(t,x) \right)_i - \tilde{q}_i(t,x) \right) \qquad (30c)$$

$$\tilde{\rho}_i(0,x) = \int_W \tilde{g}_{0,i}(t,x,w)dw, \qquad (30d)$$

$$\tilde{q}_i(0,x) = \int_W w \, \tilde{g}_{0,i}(t,x,w)dw. \qquad (30e)$$

The system (30) is hyperbolic for $\tilde{\rho}_i > 0$.

Let the random fields $(\rho, q) = (\rho, q)(t,x,\xi) : \mathbb{R}^+ \times \mathbb{R} \times \Omega \to \mathbb{R}^2$ be a pointwise a.e. solution with second moments w.r.t. to ξ of the stochastic Aw–Rascle–Zhang system with random initial data:

$$\partial_t \rho + \partial_x(q - \rho h(\rho)) = 0, \qquad (31a)$$

$$\partial_t q + \partial_x\left(\frac{q^2}{\rho} - qh(\rho) \right) = \frac{1}{\epsilon}\left(\rho V_{eq}(\rho) + \rho h(\rho) - q \right), \qquad (31b)$$

$$\rho(0,x,\xi) = \rho_0(x,\xi), \; q(0,x,\xi) = q_0(x,\xi). \qquad (31c)$$

Under the previous assumptions on the base functions $\{ \phi_0, \ldots, \phi_K \}$ and provided that for all $i = 0, \ldots, K$

$$\int_\Omega \rho_0(x,\xi)\phi_i(\xi)p_\Xi d\xi = \int_W \tilde{g}_{0,i}(t,x,w)dw, \; \int_\Omega q_0(x,\xi)\phi_i(\xi)p_\Xi d\xi = \int_W w\tilde{g}_{0,i}(t,x,w)dw, \qquad (32)$$

we have

$$G_K\left(\rho(t,x,\cdot) \right)(\xi) = \sum_{i=0}^K \tilde{\rho}_i(t,x)\phi_i(\xi) \; and \; G_K\left(q(t,x,\cdot) \right)(\xi) = \sum_{i=0}^K \tilde{q}_i(t,x)\phi_i(\xi), \qquad (33)$$

where $(\tilde{\rho}, \tilde{q})$ fulfill equation (30).

Some remarks are in order. The assumption (29) is a closure relation and has been presented in the deterministic case [24]. The result on hyperbolicity of the system (30) has been presented in [19]. Therein, also the system for the coefficients $\tilde{\rho}, \tilde{q}$ of a gPC expansion of the stochastic case of (6) has been derived, i.e., the system (30). Condition (32) states the consistency of initial data of both systems.

Proof. The proof is similar to [24] and given here for completeness. For a pointwise a.e. solution $\tilde{g}$ and corresponding densities $\tilde{\rho}$ and fluxes $\tilde{q}$ according to (19)–(20) we obtain for each $i \in \{0, \ldots, K\}$ by (22) and after integration on W

$$\partial_t \int_W \tilde{g}_i(t,x,w)dw + \partial_x \int_W w\tilde{g}_i(t,x,w) - \Big(\mathcal{P}(h(\tilde{\rho}(t,x)))\tilde{g}(t,x,w)\Big)_i dw \qquad (34)$$

$$= \frac{1}{\varepsilon}\left(\int_W \tilde{M}_i(w;\tilde{\rho}(t,x)) - \tilde{g}_i(t,x,w)dw\right). \qquad (35)$$

Since $\tilde{g} \to \mathcal{P}(\tilde{\rho})\tilde{g}$ is linear and by equation (UM1) of Lemma 2.1

$$\partial_t \tilde{\rho}_i(t,x) + \partial_x \left(\tilde{q}_i(t,x) - \Big(\mathcal{P}(h(\tilde{\rho}(t,x)))\tilde{\rho}(t,x)\Big)_i\right) = 0. \qquad (36)$$

Furthermore, we integrate (22) w.r.t. to $w\,dw$ on W to obtain

$$\partial_t \int_W w\tilde{g}_i(t,x,w)dw + \partial_x \int_W w^2\tilde{g}_i(t,x,w) - w\Big(\mathcal{P}(h(\tilde{\rho}(t,x)))\tilde{g}(t,x,w)\Big)_i dw \quad (37)$$

$$= \frac{1}{\varepsilon}\left(\int_W w\widetilde{M}_i(w;\tilde{\rho}(t,x)) - w\tilde{g}_i(t,x,w)dw\right). \qquad (38)$$

This yields

$$\partial_t \tilde{q}_i(t,x) + \partial_x \int_W w^2\tilde{g}_i(t,x,w)dw - \Big(\mathcal{P}(h(\tilde{\rho}(t,x)))\tilde{q}(t,x)\Big)_i \qquad (39)$$

$$= \frac{1}{\varepsilon}\left(\int_W w\widetilde{M}_i(w;\tilde{\rho}(t,x))dw - \tilde{q}_i(t,x)\right). \qquad (40)$$

Using now (29) and equation (28) of Lemma 2.1 we obtain the momentum equation of the second–order traffic flow model (30).

Under the assumptions (A1)–(A3) we obtain that (30) is hyperbolic as proven in [19]. Therein, also the assertion (33) has been established. □

Remark 1. Introducing stochasticity also allows for more general Maxwellians. In particular, the Maxwellian M_g could also depend on ξ directly. Hence, we may assume that

$$M_g(w;\rho,\xi) := M(w;\rho(t,x,\xi),\xi). \qquad (41)$$

The previous derivation can be also conducted for Maxwellians of the previous type. In order to conserve mass it is necessary to assume that M fulfills (UM1). Then, we obtain a gPC expansion in coefficients $\bar{\rho} = (\bar{\rho}_i)_{i=0}^K$ and $\bar{q} = (\bar{q}_i)_{i=0}^K$ as

$$\partial_t \bar{\rho}_i(t,x) + \partial_x \left[\bar{q}_i(t,x) - (\mathcal{P}(\bar{\rho}(t,x))\bar{\rho}(t,x))_i\right] = 0 \qquad (42a)$$

$$\partial_t \bar{q}_i(t,x) + \partial_x \left[\int_W w^2\bar{g}_i(t,x,w)\,dw - (\mathcal{P}(\bar{\rho}(t,x))\bar{q}(t,x))_i\right] = \frac{1}{\epsilon}\left(\int_W w\overline{M}_i\,dw - \bar{q}_i(t,x)\right) \qquad (42b)$$

$$\bar{\rho}_i(0,x) = \tilde{\rho}_i(0,x)\ \bar{q}(0,x) = \tilde{q}_i(0,x),\ \overline{M}_i = \int_\Omega M(w;\rho(t,x,\xi),\xi)\phi_i(\xi)p_\Xi(\xi)d\xi. \qquad (42c)$$

Clearly, applying assumption (29) leads for the transport part of the system the same flux as for the Aw–Rascle–Zhang system. A direct identification of the source term with fluid dynamic quantities is no longer possible but depends on the precise dependence of M on ρ and ξ.

2.2. **Stability analysis.** We extend the stability analysis [24, Section 3.2] to the stochastic case. Recall, the stochastic PDE (13) for the random field $g = g(t, x, w, \xi)$ is given by

$$\partial_t g(t, x, w, \xi) + \partial_x \Big[(w - h(\rho(t, x, \xi))) g(t, x, w, \xi) \Big] = \frac{1}{\varepsilon} \Big(M_g(w; \rho) - g(t, x, w, \xi) \Big), \tag{43}$$

where we assume that M_g fulfills (M1) and (M2). The stability analysis in [24] is based on a Chapman Enskog expansion of g in terms of ϵ. Here, we similarly assume that

$$g(t, x, w, \xi) = M_g(w; \rho(t, x, \xi)) + \varepsilon g_1(t, x, w, \xi), \tag{44}$$

where a.e. (x, w) and a.s. in ξ

$$\int_W g_1(t, x, w, \xi) dw = 0. \tag{45}$$

Up to terms of order ϵ^2 the perturbation g_1 fulfills

$$g_1(t, x, w, \xi) = -\partial_t M_g(w; \rho(t, x, \xi)) - \partial_x (w - h(\rho(t, x, \xi))) M_g(w; \rho(t, x, \xi)). \tag{46}$$

The formal computations presented in [24, Section 3.2] extend to the above equations (43) and (46) since they only rely on integration with respect to w and the properties (M1) and (M2). Those are independent of ξ. Hence, after integrating (43) with respect to w, substituting g_1 by (46) as well as subsequent differentiation leads to

$$\partial_t \rho + \partial_x \left(\rho V_{eq}(\rho) \right) = \epsilon \partial_x \left(-D(\rho) \partial_x \rho + \partial_x \int_W w^2 M_g(w, \rho) dw \right), \tag{47}$$

$$D(\rho) = \left(\partial_\rho Q_{eq}(\rho) + \partial_\rho (h(\rho)\rho) \right) \left(\partial_\rho Q_{eq}(\rho) + h(\rho) \right) + \partial_\rho h(\rho) \left(Q_{eq}(\rho) + h(\rho)\rho \right) \tag{48}$$

$$Q_{eq}(\rho) = V_{eq}(\rho)\rho, \tag{49}$$

where $\rho = \rho(t, x, \xi)$. In [24] it is assumed that the Maxwellian M_f, see Section 2, and M_g are related. In this case

$$M_f(v, \rho) := M_g(v + h(\rho), \rho) \ \forall v \in V, \rho \geq 0, \tag{50}$$

where M_f is a Maxwellian such that $\int_V M_f(v, \rho) dv = \rho$ and $\int_V v M_f(v, \rho) dv = Q_{eq}(\rho)$. Using those properties equation (47) simplifies and we obtain

$$\partial_t \rho + \partial_x \left(\rho V_{eq}(\rho) \right) = \epsilon \partial_x \left(\mu(\rho) \partial_x \rho \right), \tag{51}$$

$$\mu(\rho) = \left(-\partial_\rho Q_{eq}(\rho)^2 - \partial_\rho h(\rho) \partial_\rho Q_{eq}(\rho) \rho + Q_{eq}(\rho) \partial_\rho h(\rho) \right) + \int_V v^2 \partial_\rho M_f(v, \rho) dv. \tag{52}$$

Note that in the presented case μ is in fact a random field through its dependence on $\rho = \rho(t, x, \xi)$. Therefore, compared with the deterministic case, we may now infer information on e.g. expectation, confidence bands or the probability of μ to be non-positive. In particular, the later is relevant for qualitative assessment of

traffic flow since it shows where possible instabilities may occur. Hence, for fixed $t \geq 0$ and $x \in \mathbb{R}$ consider

$$\mathbb{P}_{t,x}(\mu \leq 0) := \int_{\Omega} H(-\mu(\rho(t,x,\xi))p_{\Xi}(\xi)d\xi. \tag{53}$$

It has been argued in [24] that (53) indicates regions of traffic situations of high risk. Further, points (t,x) where $\mathbb{P}_{t,x}(\cdot) > 0$ holds might lead to the rise of stop–and–go waves. A numerical investigation of (53) will be presented in the forthcoming section.

Note that the computation of (53) requires to reconstruct the stochastic field $\rho(t,x,\xi)$. This can be obtained by reconstruction of g given by (16) where $\tilde{g}$ are given by equation (22).

For particular choices of $V_{eq}(\cdot)$ and $h(\cdot)$ the gPC expansion of the first terms in μ can be obtained directly using the moments $\tilde{\rho}$. In fact, assume $h(\rho) = \rho$ and $V_{eq} = \rho_{max} - \rho$. Then, $Q_{eq} = \rho(\rho_{max} - \rho)$ is the flux of the Lighthill-Whitham–Richards model and equation (51) simplifies

$$\mu(\rho) = R(\rho) + \int_V v^2 \partial_\rho M_f(v,\rho)dv, \tag{54}$$

$$R(\rho) := -(\rho_{max} - 2\rho)^2 - (\rho_{max}\rho - \rho^2) + \rho(\rho_{max} - \rho). \tag{55}$$

Hence, we obtain

$$G_K(R(\rho(t,x,\cdot)))(\xi) = \sum_{i=0}^{K} \tilde{R}_i(t,x)\phi_i(\xi) \tag{56}$$

where $\tilde{R}$ is expressed in terms of $\tilde{\rho}$ and $1\!\!\!/ = (1,\ldots,1)^T \in \mathbb{R}^{K+1}$

$$\tilde{R}(t,x) = -P(\rho_{max}1\!\!\!/ - 2\tilde{\rho})(\rho_{max}1\!\!\!/ - 2\tilde{\rho}) - \rho_{max}\tilde{\rho} + P(\tilde{\rho})\tilde{\rho} + P(\tilde{\rho})(\rho_{max}1\!\!\!/ - \tilde{\rho}) \tag{57}$$

However, in the numerical simulations we use a Maxwellian M_f obtained by a discrete velocity model, see below for the details. Therein, ρ enters within a rational polynomial and a simple expression as above, also for the expansion of $\partial_\rho M_f(v,\rho)dv$, seems to be not possible.

3. **Computation results.** Numerically, we are interested in indicating and forecast regions of high risk of congestion or instabilities. For this reason we focus on the simulation of (53). First, we perform a steady state analysis and investigate parameters influencing regions of high probability. Secondly, we show the evolution of this probability in time.

As Maxwellian we choose a discrete velocity distribution with n_v velocities as in [24]:

$$M_f(v;\rho) = \sum_{j=1}^{n_v} f_j^{\infty}(\rho)\delta_{v_j}(v). \tag{58}$$

The weights are normalized to ensure equation (27), i.e., $\sum_{j=1}^{n_v} f_j^{\infty}(\rho) = \rho$ for any $\rho > 0$. The set of velocities is $\{v_j\}_{j=1}^{n_v}$. Then, for fixed $\rho > 0$ the weights are recursively defined by

$$f_j^\infty = \begin{cases} 0 & \rho \geq \frac{1}{2}, \\ \frac{-2(1-\rho)\sum_{k=1}^{j-1} f_k^\infty + (1-2\rho)\rho + \sqrt{[(1-2\rho)\rho - 2(1-\rho)\sum_{k=1}^{j-1} f_k^\infty]^2 + 4\rho(1-\rho)\rho f_k^\infty}}{2(1-\rho)} & else \end{cases},$$

(59)

$$j = 1, \ldots, n_v - 1,$$

$$f_{n_v}^\infty = \rho - \sum_{j=1}^{n_v-1} f_j^\infty. \tag{60}$$

We use $V_{eq} = 1 - 2\rho$ and $h(\rho)$ as indicated in the tests below. The Maxwellian M_g is obtained through relation (50). Since the previous Maxwellian is a rational polynomial of ρ, an explicit expression of $\mu(\cdot)$ in terms of the moments of ρ might not be feasible. Therefore, we evaluate (53) numerically using quadrature with N_ξ number of points.

The gPC Aw–Rascle–Zhang system is discretized as in [19], i.e., employing a local Lax Friedrichs scheme to solve (30).

The numerical parameters are as follows. We consider the space interval $x \in [a, b] = [0, 2]$ and define the uniform spatial grid of size $\Delta x = 2 \cdot 10^{-2}$. Moreover, let $T_f = 1$ be the final time of the simulations and Δt the time step, which is chosen in such a way that the CFL condition is fulfilled. By N_t we denote the number of the time steps needed to reach T_f. The random variable ω is assumedto be uniform distributed on $(0, 1)$, i.e., $p_\Xi = 1$ and $\Omega = (0, 1)$. As basis functions we consider the Haar basis, which are known to fulfill (A1)–(A3). The numerical quadrature of (53) is conducted with a uniform discretization of $(0, 1)$ in ξ with $N_\xi = 10^4$ quadrature nodes. Whenever necessary the random fields density and flux are approximated up to a specified order K by $\rho(t, x, \xi) = \sum_{i=0}^{K} \tilde{\rho}_i(t, x)\phi_i(\xi)$ and similarly for $q(t, x, \xi)$.

3.1. **Steady state analysis.** The Maxwellian M_f depends on two parameters, the number of discrete velocities n_v governing the level of description of traffic as well as the local density $0 < \rho < 1$. In the steady state case the density ρ has been a constant in the deterministic case [24], however, it is now a random parameter. Since we are interested in the stability of traffic patterns we setup the steady state problem as follows: We assume a constant traffic density ρ_0 that is perturbed by a (possibly small) perturbation

$$\rho(\xi) = \rho_0 + \sigma(\xi - \frac{1}{2}), \tag{61}$$

where $\sigma > 0$ controls the standard deviation and the factor $\frac{1}{2}$ is included to have zero mean for ξ uniformly distributed. We are interested in the probability (53) for the previous choice of ρ and $\rho_0 \in [0.1; 0.9]$ with $\sigma = 0.1$. The resulting $\mathbb{P}(\mu \leq 0)$ is shown in Figure 2 (red curve).

In the free flow regime, i.e., $\rho_0 < \frac{1}{2}$, the probability of instabilities is zero, it is increasing until its maximum transition regime, and decreasing in the congested are $\rho > \frac{1}{2}$. It is interesting to observe that in the congested region the probability of $\mu < 0$ is close to zero with the interpretation that the traffic propagates at low speed and and no free space to accelerate. As expected, the highest probability for instabilities is in the transitional regime $\rho_0 \approx (0.5, 0.6)$.

Moreover, in Figure 2, we compare the predictions for $n_v = 3$ and $n_v = 10$. In case of a small and large number of discrete velocities. In case of only three
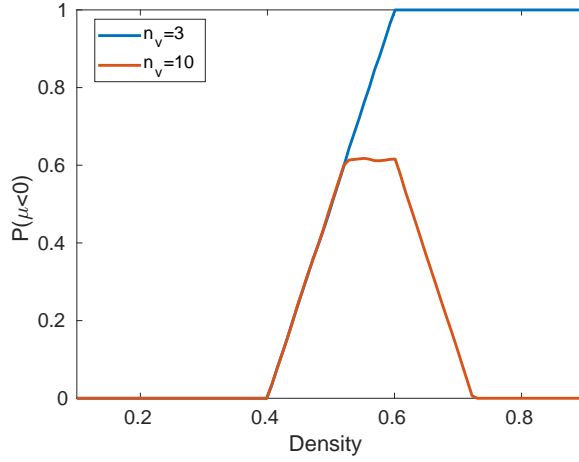
FIGURE 2. Probability (53) for a Maxwellian M_f with different number of discrete velocities: $n_v = 3$, $n_v = 10$. On the x-axis ρ_0 is shown, see (61).

velocities the transition region stretches up to the maximal density due to the limit choices of velocities the drivers can attain. For $n_v = 10$, we observe the highest probability for ρ between 0.5 and 0.6 as detailed above.

Further, the dependence of $\mathbb{P}(\mu < 0)$ for fixed values of ρ_0 but different standard deviations σ is shown. We observe a different behavior if we start from $\rho_0 = 0.4$ and $\rho_0 = 0.6$, see Figure 3.
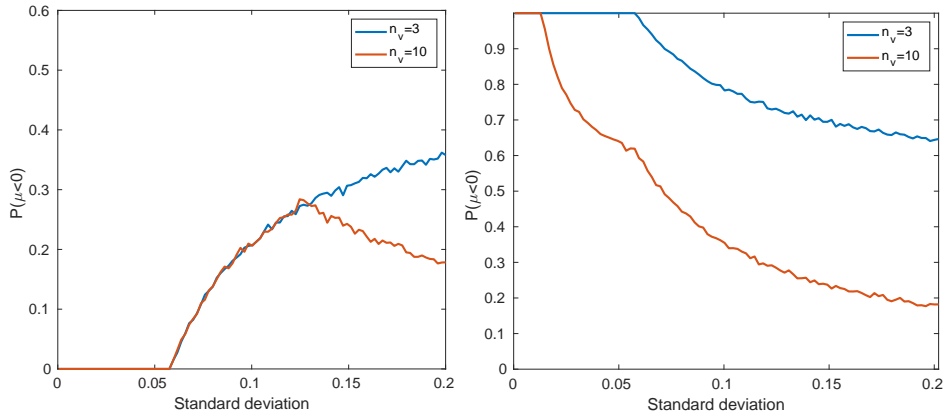
FIGURE 3. Probability (53) for different velocities samples: $n_v = 3$ (blue line), $n_v = 10$(red line) for different values of $\rho_0 = 0.4$(left) $\rho_0 = 0.6$(right) when the standard deviation σ ranges from zero to 0.2.

In the latter, the probability is decreasing with the possible explanation that the density is spreading far from the transition area. In the former, we are in the opposite situation, since we approach the transition region for increasing value for the standard deviation.

Furthermore, we compare also the effect of different hesitation functions. In Figure 4, $h(\rho) = \rho$ (blue line) and $h(\rho) = \rho^3$ are considered. The observed behavior is very similar.
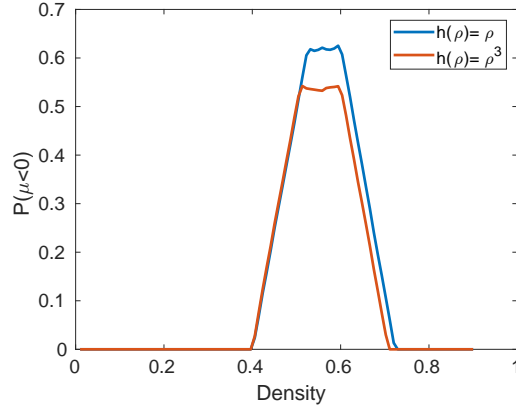

FIGURE 4. Probability (53) for different hesitation functions: $h(\rho) = \rho$ (blue line) and $h(\rho) = \rho^3$ (red line).

3.2. **Time–dependent problems.** We investigate numerically if the dynamics amplifies the probability of instabilities starting from a Riemann problem. In order to evaluate (53) for a temporal and spatially dependent ρ, we need to reconstruct the density and therefore we first show the convergence in K. In all following computations we set $n_v = 5$, $N_\xi = 10^2$ and define the Riemann problem:

$$\rho(x, 0, \xi) = \begin{cases} \rho_l \equiv \xi \sim \mathcal{U}(0.55, 0.85) & x < 1 \\ 0.2 & x \geq 1 \end{cases}, \qquad v(x, 0, \xi) = \begin{cases} 0.2 & x < 1 \\ 0.7 & x \geq 1 \end{cases}.$$
$$(62)$$

First of all, we show the behavior of the mean and the variance of the density for different values of K, which play a crucial role for computing μ. In Fig. 5 we observe a convergence for increasing K both in the mean and in the variance at $t = T_f$ and initial data (62).
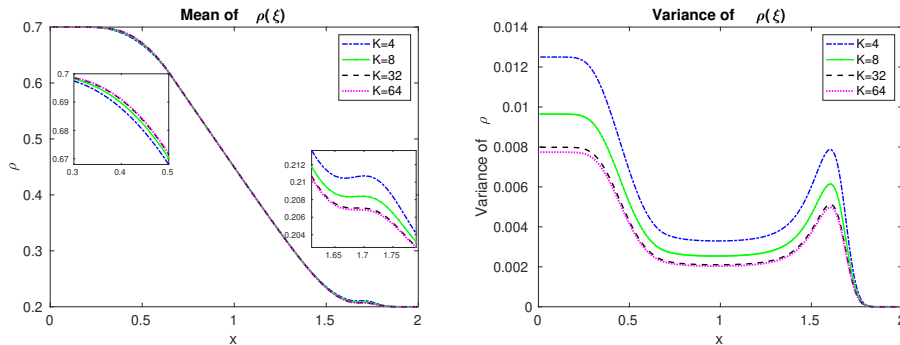

FIGURE 5. Mean and variance of the density at $t = T_f$ for different .

In Figure 6 we show $\mathbb{P}_{T_f,x}(\mu < 0)$ for an increasing number of base functions K.
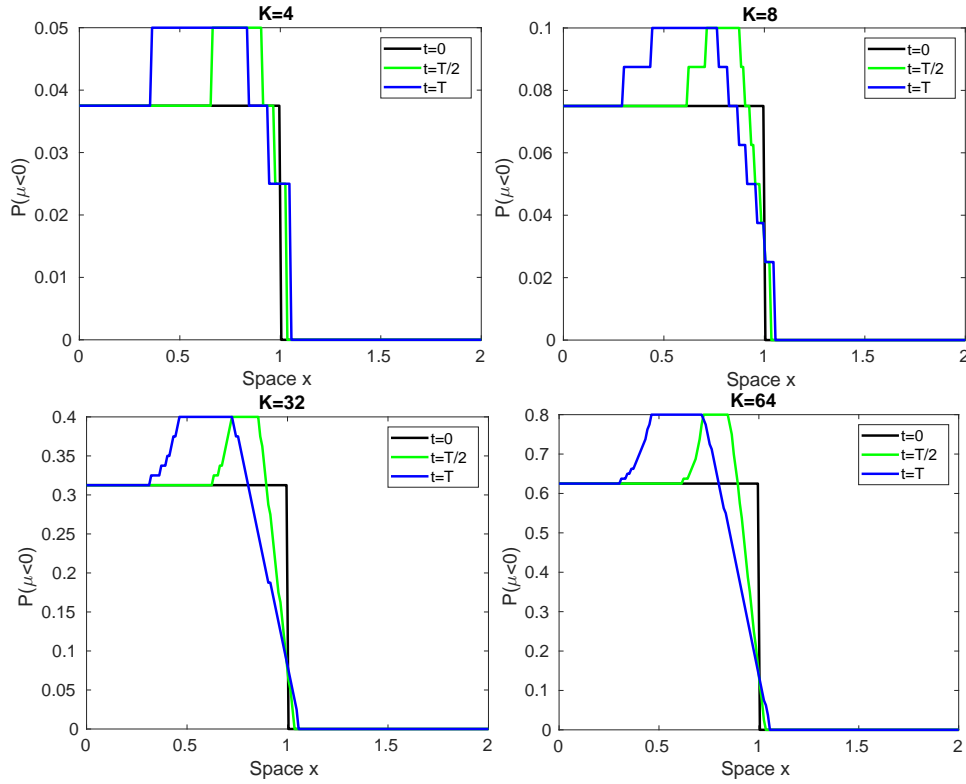

FIGURE 6. Probability (53) at time $t = 0$ (black line), $t = \frac{T_f}{2}$ (green line) $t = T$ (blue line) for $K = 4$ (top-left), $K = 8$ (top-right), $K = 32$ (bottom-left), $K = 64$ (bottom-right).

Moreover, the probability of instabilities is increasing in time and travels backward. As explanation of this behavior we note that the given data leads to a rarefaction wave in (t, x) for any fixed ρ_l. Hence, drivers observe a free flow area ahead and accelerate. The 95%−confidence band of the density ρ at the final time T_f is shown in Figure 7(right).

As second test case we consider a (random) shock wave as given by (63). Here, the probability of instabilities increases and spreads both forward and backward. A possible explanation might be that the vehicles have to decelerate in order to avoid collisions leading also to backwards spreading waves.

$$\rho(x, 0, \xi) = \begin{cases} \rho_l \equiv \xi \sim \mathcal{U}(0.15, 0.45) & x < 1 \\ 0.75 & x \geq 1 \end{cases}, \qquad v(x, 0, \xi) = \begin{cases} 0.7 & x < 1 \\ 0.3 & x \geq 1 \end{cases}.$$
(63)

In Figure 8(right) the 95%−confidence band of the density at the final time T_f is shown. It is interesting to note that even starting from $\mathbb{P}(\mu < 0) \equiv 0$ does not ensure to avoid instabilities as time evolves, see Figure 8(left). Indeed, at time $t = 0$ the probability is zero. However, as the time evolves, the density enters the transition phase and the probability of instability grows.
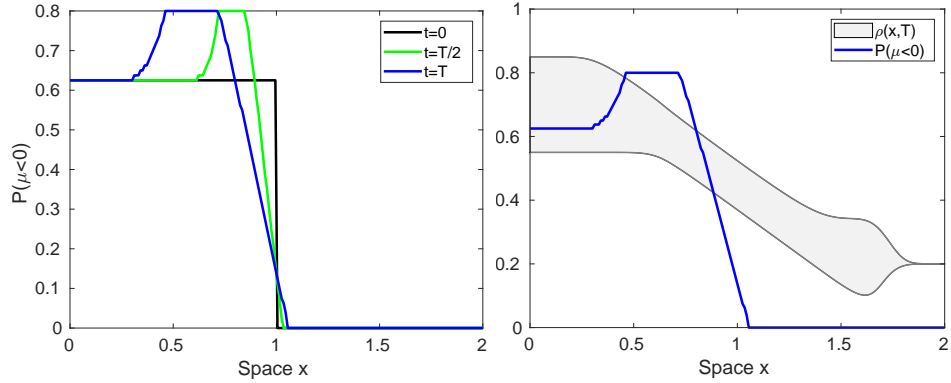
FIGURE 7. Probability of negative diffusion coefficient in a rarefaction case at different time: $t = 0$, $t = \frac{T_f}{2}$, $t = T_f$, $K = 64$, and comparison with the confident region of the density at $t = T_f$.
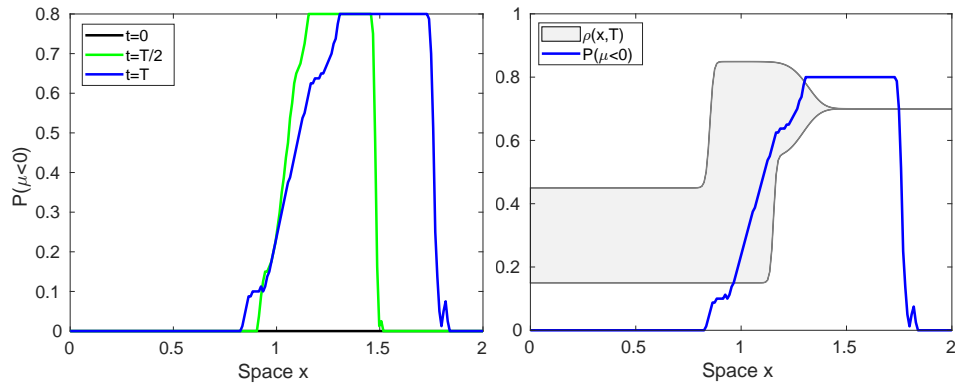

FIGURE 8. Density profile and probability of negative diffusion coefficient in a shock case at $t = T_f$, $K = 64$.

REFERENCES

[1] A. Aw and M. Rascle, Resurrection of "second order" models of traffic flow, *SIAM J. Appl. Math.*, **60** (2000), 916–938.

[2] I. Babuška, F. Nobile and R. Tempone, A stochastic collocation method for elliptic partial differential equations with random input data, *SIAM J. Numer. Anal.*, **45** (2007), 1005–1034.

[3] M. Bando, K. Hasebe, A. Nakayama, A. Shibata and Y. Sugiyama, Dynamical model of traffic congestion and numerical simulation, *Phys. Rev. E*, **51** (1995), 1035–1042.

[4] N. Bellomo and C. Dogbe, On the modeling of traffic and crowds: A survey of models, speculations, and perspectives, *SIAM Rev.*, **53** (2011), 409–463.

[5] P. L. Bhatnagar, E. P. Gross and M. Krook, A model for collision processes in gases. i. small amplitude processes in charged and neutral one-component systems, *Phys. Rev.*, **94** (1954), 511–525.

[6] R. Borsche and A. Klar, A nonlinear discrete velocity relaxation model for traffic flow, *SIAM J. Appl. Math.*, **78** (2018), 2891–2917.

[7] R. H. Cameron and W. T. Martin, The orthogonal development of non-linear functionals in series of Fourier-Hermite functionals, *Ann. of Math.*, **48** (1947), 385–392.

[8] J. Carrillo, L. Pareschi and M. Zanella, Particle based gPC methods for mean-field models of swarming with uncertainty, *Commun. Comput. Phys.*, **25** (2019), 508–531.

[9] J. Carrillo and M. Zanella, Monte Carlo gPC methods for diffusive kinetic flocking models with uncertainties, *Vietnam J. Math.*, **47** (2019), 931–954.

[10] Q.-Y. Chen, D. Gottlieb and J. S. Hesthaven, Uncertainty analysis for the steady-state flows in a dual throat nozzle, *J. Comput. Phys.*, **204** (2005), 378–398.

[11] R. M. Colombo, Hyperbolic phase transitions in traffic flow, *SIAM J. Appl. Math.*, **63** (2002), 708–721.

[12] E. Cristiani and S. Sahu, On the micro-to-macro limit for first-order traffic flow models on networks, *Netw. Heterog. Media*, **11** (2016), 395–413.

[13] B. J. Debusschere, H. N. Najm, P. P. Pébay, O. M. Knio, R. G. Ghanem and O. P. L. Maître, Numerical challenges in the use of polynomial chaos representations for stochastic processes, *SIAM J. Sci. Comput.*, **26** (2004), 698–719.

[14] B. Després, G. Poëtte and D. Lucor, Uncertainty quantification for systems of conservation laws, *J. Comput. Phys.*, **228** (2009), 2443–2467.

[15] M. Di Francesco and M. D. Rosini, Rigorous derivation of nonlinear scalar conservation laws from follow-the-leader type models via many particle limit, *Arch. Ration. Mech. Anal.*, **217** (2015), 831–871.

[16] S. Fan, M. Herty and B. Seibold, Comparative model accuracy of a data-fitted generalized Aw-Rascle-Zhang model, *Netw. Heterog. Media*, **9** (2014), 239–268.

[17] D. Gazis, R. Herman and R. Rothery, Nonlinear follow-the-leader models of traffic flow, *Oper. Res.*, **9** (1961), 545–567.

[18] S. Gerster and M. Herty, Entropies and symmetrization of hyperbolic stochastic Galerkin formulations, *Commun. Comput. Phys.*, **27** (2020), 639–671.

[19] S. Gerster, M. Herty and E. Iacomini, Stability analysis of a hyperbolic stochastic galerkin formulation for the aw-rascle-zhang model with relaxation, *Math. Biosci. Eng.*, **18** (2021), 4372–4389.

[20] S. Gerster, M. Herty and A. Sikstel, Hyperbolic stochastic Galerkin formulation for the p-system, *J. Comput. Phys.*, **395** (2019), 186–204.

[21] D. Gottlieb and D. Xiu, Galerkin method for wave equations with uncertain coefficients, *Commun. Comput. Phys.*, **3** (2008), 505–518.

[22] M. Herty and R. Illner, Analytical and numerical investigations of refined macroscopic traffic flow models, *Kinet. Relat. Models*, **3** (2010), 311–333.

[23] M. Herty and L. Pareschi, Fokker-Planck asymptotics for traffic flow models, *Kinet. Relat. Models*, **3** (2010), 165–179.

[24] M. Herty, G. Puppo, S. Roncoroni and G. Visconti, The BGK approximation of kinetic models for traffic, *Kinet. Relat. Models*, **13** (2020), 279–307.

[25] H. Holden and N. H. Risebro, The continuum limit of Follow-the-Leader models—a short proof, *Discrete Contin. Dyn. Syst.*, **38** (2018), 715–722.

[26] J. Hu and S. Jin, A stochastic Galerkin method for the Boltzmann equation with uncertainty, *J. Comput. Phys.*, **315** (2016), 150–168.

[27] S. Jin and Y. Zhu, Hypocoercivity and uniform regularity for the Vlasov-Poisson-Fokker-Planck system with uncertainty and multiple scales, *SIAM J. Math. Anal.*, **50** (2018), 1790–1816.

[28] A. Klar and R. Wegener, A kinetic model for vehicular traffic derived from a stochastic microscopic model, *Transport. Theor. Stat.*, **25** (1996), 785–798.

[29] A. Klar and R. Wegener, Enskog-like kinetic models for vehicular traffic, *J. Stat. Phys.*, **87** (1997), 91–114.

[30] J. Kusch, G. Alldredge and M. Frank, Maximum-principle-satisfying second-order intrusive polynomial moment scheme, *SMAI J. Comput. Math.*, **5** (2019), 23–51.

[31] O. P. Le Maître and O. M. Knio, *Spectral Methods for Uncertainty Quantification*, Springer, New York, 2010.

[32] P. L'Ecuyer and C. Lemieux, Recent advances in randomized quasi-monte carlo methods, In *Internat. Ser. Oper. Res. Management Sci.*, **46** (2002), 419–474.

[33] M. J. Lighthill and G. B. Whitham, On kinematic waves. II. A theory of traffic flow on long crowded roads, *Proc. Roy. Soc. London. Ser. A*., **229** (1955), 317–345.

[34] O. P. L. Maître and O. M. Knio, *Spectral Methods for Uncertainty Quantification*, Springer Netherlands, 1 ed., 2010.

[35] P. Pettersson, G. Iaccarino and J. Nordström, A stochastic Galerkin method for the Euler equations with Roe variable transformation, *J. Comput. Phys.*, **257** (2014), 481–500.

[36] P. Pettersson, G. Iaccarino and J. Nordström, *Polynomial Chaos Methods for Hyperbolic Partial Differential Equations*, Numerical techniques for fluid dynamics problems in the presence of uncertainties. Mathematical Engineering. Springer, Cham, 2015.

[37] R. Pulch and D. Xiu, Generalised polynomial chaos for a class of linear conservation laws, *J. Sci. Comput.*, **51** (2012), 293–312.

[38] G. Puppo, M. Semplice, A. Tosin and G. Visconti, Kinetic models for traffic flow resulting in a reduced space of microscopic velocities, *Kinet. Relat. Mod.*, **10** (2017), 823–854.

[39] B. Seibold, M. R. Flynn, A. R. Kasimov and R. R. Rosales, Constructing set-valued fundamental diagrams from jamiton solutions in second order traffic models, *Netw. Heterog. Media*, **8** (2013), 745–772.

[40] R. Shu, J. Hu and S. Jin, A stochastic Galerkin method for the Boltzmann equation with multi-dimensional random inputs using sparse wavelet bases, *Numer. Math. Theory Methods Appl.*, **10** (2017), 465–488.

[41] T. J. Sullivan, *Introduction to Uncertainty Quantification*, Texts in Applied Mathematics, 63. Springer, Cham, 2015.

[42] K. Taimre, Botev, *Handbook of Monte Carlo Methods*, John Wiley and Sons, 2011.

[43] A. Tosin and M. Zanella, Boltzmann-type models with uncertain binary interactions, *Commun. Math. Sci.*, **16** (2018), 963–985.

[44] A. Tosin and M. Zanella, Uncertainty damping in kinetic traffic models by driver-assist controls, *Math. Control Relat. Fields*, **11** (2021), 681–713.

[45] N. Wiener, The homogeneous chaos, *Amer. J. Math.*, **60** (1938), 897–936.

[46] D. Xiu, *Numerical Methods for Stochastic Computations: A Spectral Method Approach*, Princeton University Press, Princeton, N.J, 2010.

[47] D. Xiu and G. E. Karniadakis, The Wiener-Askey polynomial chaos for stochastic differential equations, *SIAM J. Sci. Comput.*, **24** (2002), 619–644.

[48] M. Zanella, Structure preserving stochastic Galerkin methods for Fokker-Planck equations with background interactions, *Math. Comput. Simulation*, **168** (2020), 28–47.

[49] H. M. Zhang, *A non-equilibrium traffic model devoid of gas-like behavior*, *Transport. Res. B-Meth.*, **36** (2002), 275–290.

[50] Y. Zhu and S. Jin, The Vlasov-Poisson-Fokker-Planck system with uncertainty and a one-dimensional asymptotic preserving method, *Multiscale Model. Simul.*, **15** (2017), 1502–1529.

E-mail address: herty@igpm.rwth-aachen.de
E-mail address: iacomini@igpm.rwth-aachen.de